A High Step-up Modular Isolated DC-DC Converter for Large Capacity Photovoltaic Generation System integrated into MVDC Grids

Shilei Lu[1], Kai Sun[1], Guoen Cao[2], Yongdong Li[1], Jung-Ik Ha[3], and Geon-Hong Min[3]
[1] State Key Lab of Power Systems, Department of Electrical Engineering, Tsinghua University, Beijing, China
[2] Institute of Electrical Engineering, Chinese Academy of Sciences, Beijing, China
[3] Department of Electrical and Computer Engineering, Seoul National University, Seoul, Republic of Korea

***Abstract*—Nowadays, the research and design of the DC-DC conversion system has become more and more popular in the application of photovoltaic generation into the medium voltage DC (MVDC) grids. A novel high power modular isolated DC-DC converter with high step-up ratio is proposed as a module of the DC-DC conversion system in this paper. Based on the input parallel and output series (IPOS) connections of the proposed modular converters, the system is easy to achieve high capacity and high voltage. A two-stage structure is employed in the proposed converter. The interleaved boost topology is applied to the front-stage, which realizes MPPT for PV arrays with low input current ripples. The full-bridge LLC topology is employed as the back-stage, which lowers power losses by the implementation of soft-switching. The voltage gain of the proposed converter is derived in detail. The theoretical analysis and control strategy are studied in depth. Simulation and experiment verify the feasibility and effectiveness of the proposed converter.**

***Index Terms*—DC-DC converter, high step-up converter, medium voltage DC grid, photovoltaic generation system**

I. Introduction

In the last few years, grid-connected photovoltaic (PV) power generation system has expanded significantly all over the world [1]. Nowadays, PV generation is typically connected to high voltage AC (HVAC) grids. In a HVAC grid-connected PV system, centralized inverters and LF step-up transformers are used [2]. However, the AC grid connection method and HVAC grid have some disadvantages, such as resonant problems, synchronous problems and limitation of transmission power and distance [3], [4].

Therefore, an effective solution of MVDC grid-connected PV system is introduced to overcome these shortcomings brought by HVAC grid-connected PV system [5]-[7]. MVDC grids gradually become a tendency. Furthermore, DC-DC conversion system plays the most important part in the MVDC grid-connected PV system. Generally speaking, the DC-DC conversion scheme is divided into single-stage scheme and two-stage scheme. Although the single-stage conversion scheme reduces the system size, cost and losses, it performs lower overall efficiency because of partial shading [8]. The two-stage conversion scheme can avoid this problem, thereby achieving higher efficiency with maximum power point tracking (MPPT) algorithm [9]. In consequence, a modular two-stage conversion system with novel converters in MVDC grid-connected PV generation applications is proposed in this paper. The conversion system reaches the megawatt level and the proposed converter based on SiC MOSFET features high step-up ratio, high efficiency, high power density and high frequency (HF) isolation. In order to achieve high voltage and large capacity, the proposed converter adopts an input parallel output series (IPOS) structure to form the conversion system.

II. System Configuration and the Proposed Converter

As shown in Fig. 1, the conversion system is configured as an IPOS structure to realize the integration of large-scale photovoltaic power into a MVDC grid. Thus, each converter module only needs to support one-nth of the total power (n is the number of modules). And it is easy to achieve very high voltage gain through this structure. What's more, this structure contributes to improving system stability and reliability. However, when photovoltaic power is integrated into the MVDC grid, there are not only structural requirements for the conversion system, but also higher requirements for the converter module [10].

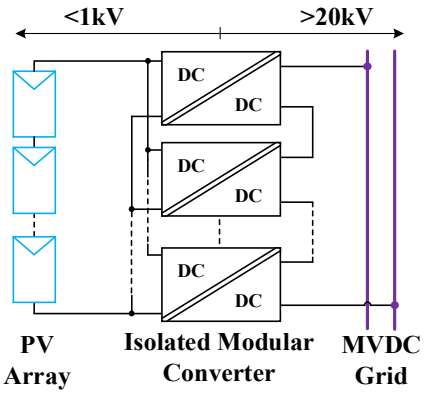

Fig. 1. MVDC grid-connected PV system

A. Requirements for the Converter Module

1) High voltage and large capacity

Photovoltaic power generation is usually integrated into the MVDC grid on a large scale and the voltage in the MVDC side is usually higher than 30kV. In addition, the number of converter modules n cannot be too much, otherwise the cost will increase and the control will become complicated. As a result, for a converter module, the requirement of high voltage and large capacity is still necessary.

2) Ultra-high step-up ratio

Generally speaking, the output voltage of PV array is typically several hundred volts due to the insulation limitations of the photovoltaic panels, whereas the output voltage of a converter module is typically several kilovolts or more. Thus, the converter module needs to have an ultra-high step-up ratio to raise the voltage and the single-stage conversion scheme is probably not applicable.

3) Electrical isolation

Isolation is usually maintained between the PV array and the MVDC grid to ensure that they do not affect each other, consequently making the system safe, reliable and stable. Moreover, in order to reduce the size and improve the power density of converters, the high frequency transformer is a very suitable candidate.

4) High efficiency and power density

As is well-known, the high efficiency and power density is vital for a converter. It has a considerable impact on economic benefit.

5) The ability to implement MPPT

It is necessary for a PV generation system to implement MPPT. It not only increases revenue and reduces investment cycles, but also increases power generation and overall efficiency.

B. The Proposed DC-DC Converter with 1:10 Ratio

In consideration of the five requirements for the converter module mentioned above, a two-stage DC-DC converter for photovoltaic generation integrated into MVDC grids is proposed, as is depicted in Fig. 2. The proposed converter is made up of two stages where the two-phase interleaved Boost topology is employed as the front-stage and the full-bridge LLC topology is employed as the back-stage. So it can be called the interleaved Boost and full-bridge LLC converter (IB-FBLLC). Both stages can achieve boost, which greatly increases the step-up ratio. The front-stage mainly takes charge of executing a MPPT algorithm and the power flow. Compared with conventional Boost converter, the interleaved structure cuts down the ripples greatly, allowing the size of filters much decrease [11]. The back-stage is mainly used to implement HF isolation and soft-switching which reduces switching losses [12]. The wide band-gap semiconductor devices SiC MOSFETs are employed as switching devices of both stages, which improves the efficiency and power density of the converter.

The typical operation waveforms of two stages are illustrated in Fig. 3. The driving of the two-phase interleaved boost front-stage employs a 180-degree phase shift modulation method. The full-bridge LLC back-stage operates at fixed frequency while switching frequency is equal to the resonant frequency. Furthermore, zero voltage switching (ZVS) and zero current switching (ZCS) come true for the switches. Meanwhile, the voltage gain of LLC back-stage is independent of the quality factor of the resonant tank [13].

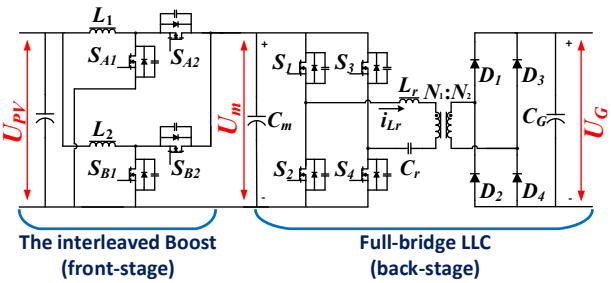

Fig. 2. The proposed IB-FBLLC converter

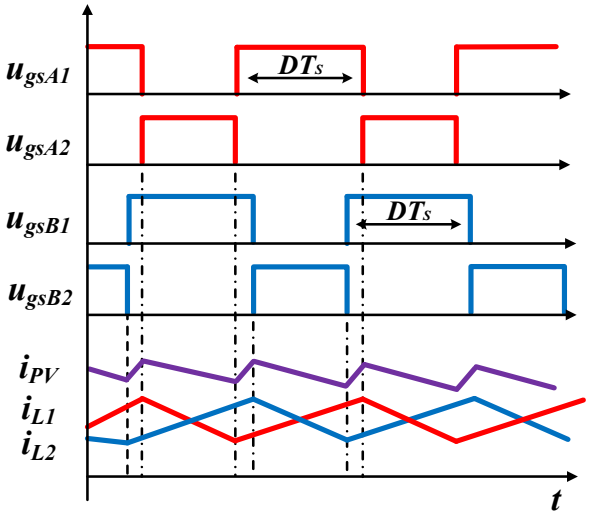

(a) Front-stage

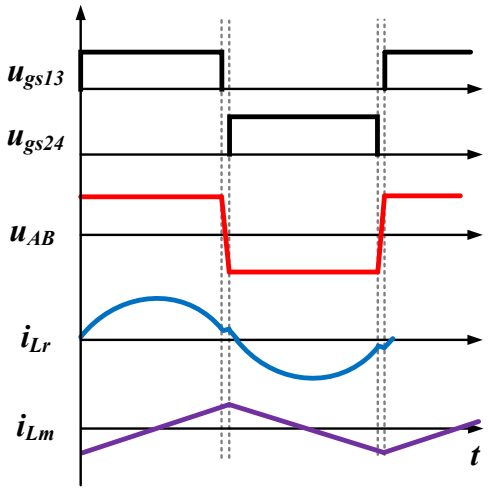

(b) Back-stage

Fig. 3. Operation waveforms of two stages

C. The Voltage Gain of IB-FBLLC

Just like the structure of the converter, the overall voltage gain can be obtained separately from the two parts.

The front-stage interleaved Boost topology typically operates in Continuous Conduction Mode (CCM). Thus,

its voltage conversion ratio is the same as that of a normal Boost converter, which is

$$M_{Pre}=\frac{U_m}{U_{PV}}=\frac{1}{1-D_{A1}} \tag{1}$$

where D_{A1} is the duty cycle of S_{A1} or S_{B1} PWM signal.

The voltage gain formula of back-stage full-bridge LLC topology can be gotten by Fundamental Harmonic Approximation (FHA). The FHA equivalent model is shown in Fig. 4 [14].

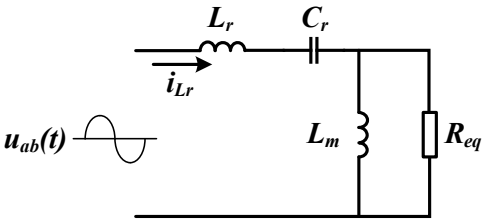

Fig. 4. The FHA equivalent model

From Fig. 4, the voltage gain of LLC stage can be derived as [15]

$$M_{Post}=\frac{U_G}{U_m}=\frac{n}{\sqrt{(1+\frac{1}{k}-\frac{1}{kf_n})^2+Q^2(f_n-\frac{1}{f_n})^2}} \tag{2}$$

$$Q=\frac{1}{R_{eq}}\sqrt{\frac{L_r}{C_r}} \tag{3}$$

$$k=\frac{L_m}{L_r} \tag{4}$$

$$f_n=\frac{f_s}{f_r} \tag{5}$$

$$f_r=\frac{1}{2\pi\sqrt{L_rC_r}} \tag{6}$$

$$R_{eq}=\frac{8n^2R_o}{\pi^2} \tag{7}$$

where n is turns ratio of the transformer, Q is the quality factor, k is the ratio of the magnetizing inductance to the resonant inductance, f_n is the normalized frequency, and R_{eq} is the equivalent resistance that is converted to the primary side.

Therefore, the voltage gain of IB-FBLLC is

$$M_{IB-FBLLC}=M_{Pre}M_{Post}=\frac{n}{(1-D_{A1})\sqrt{(1+\frac{1}{k}-\frac{1}{kf_n})^2+Q^2(f_n-\frac{1}{f_n})^2}} \tag{8}$$

The back-stage is designed to work at the resonance point f_n =1 for high efficiency in this paper. In this case, the above formula can be further simplified to

$$M_{IB-FBLLC}=\frac{n}{1-D_{A1}} \tag{9}$$

According to (8), it can be seen that the voltage gain of IB-FBLLC is determined by the duty cycle D_{A1} of front-stage and turns ratio n of the back-stage transformer. Due to the effects of both, the converter has a high step-up ratio.

III. Control Strategy of the Proposed Converter

The control diagram of IB-FBLLC converter is shown in Fig. 5. The front-stage is equipped with MPPT and power flow algorithm. In addition, perturbation and observation method is employed as a mature MPPT strategy. The back-stage works in an open loop state. In the meantime, the voltage gain of LLC back-stage is only determined by the transformer and is equal to the transformer ratio, so the intermediate voltage, that is, the output voltage of the front-stage is clamped. Hence power control can be transformed into current control. Finally, the current control is easily realized by PI regulators.

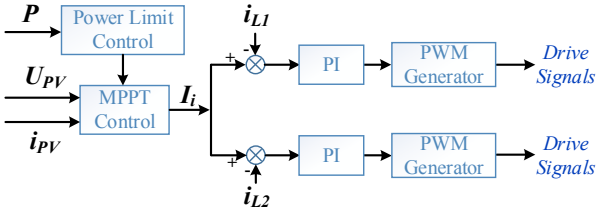

Fig. 5. Control diagram of IB-FBLLC

IV. Simulation and Experimental Verification

A. Simulation Verification

In order to validate the proposed IB-FBLLC topology and the control scheme, a simulation model is designed by MATLAB/Simulink. The detailed parameters are listed in Table I.

TABLE I
Detailed Parameters of the Simulation

Parameter	Symbol	Value
PV voltage	U_{PV}	400V~800V
Grid voltage	U_G	5kV
Turns ratio of the transformer	$N_1:N_2$	1:5
Switching frequency of the front-stage	f_B	50kHz
Switching frequency of the back-stage	f_L	50kHz
Resonant frequency	f_r	50kHz
Boost inductance	L_1, L_2	180μH
Magnetizing inductance	L_m	300μH
Resonant inductance	L_r	17μH
Resonant capacitance	C_r	0.6μF

Simulation results are shown in Fig. 6-11. When IB-FBLLC converter operates with an 80kW load, the voltage regulation is smooth and eventually stabilizes, which verifies the feasibility of the converter. When IB-FBLLC converter is integrated into MVDC grid by the control strategy mentioned in Section III, the interleaved structure, drive, resonant tank and soft-switching all perform well and act as a good effect on ripples, efficiency, power density.

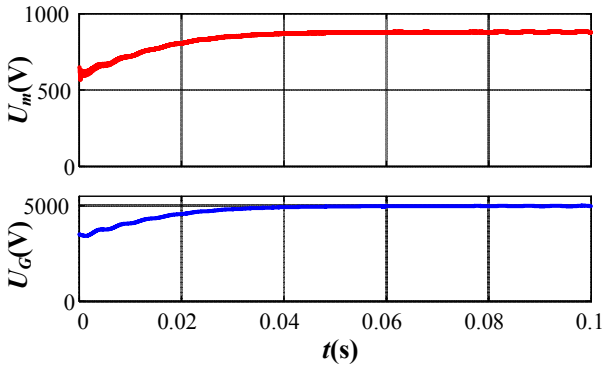

Fig. 6. The intermediate voltage and grid voltage

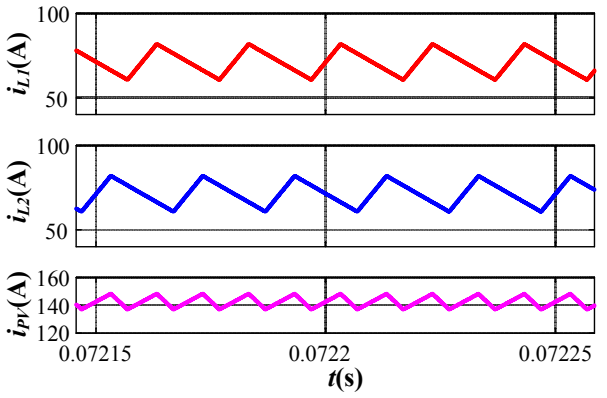

Fig. 7. Currents of both Boost inductors and PV side

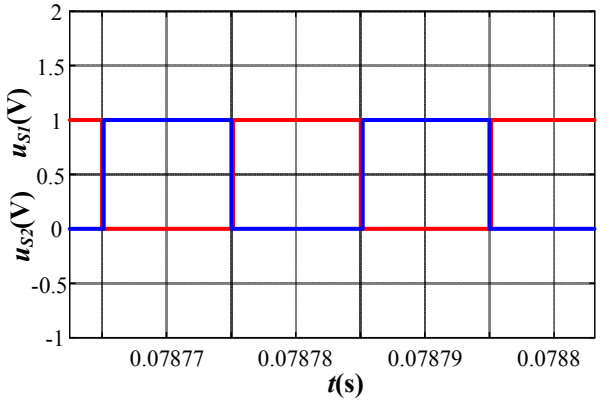

Fig. 8. Drive signal of MOSFET S_1 and S_2

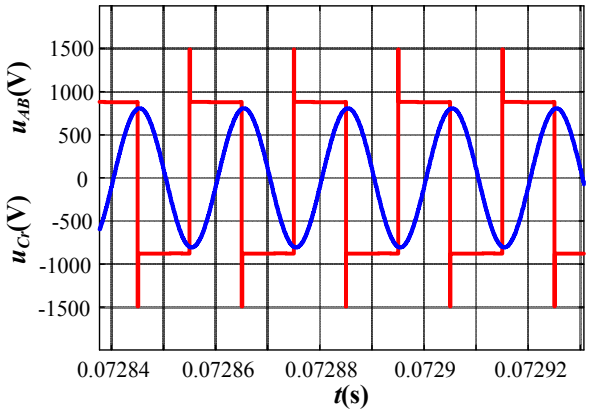

Fig. 9. Voltage between A and B and voltage across the resonant capacitor

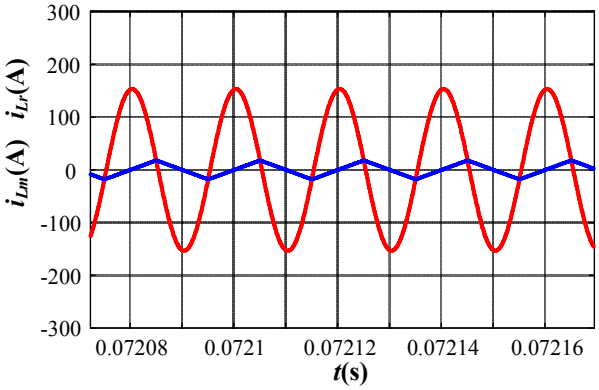

Fig. 10. Resonant current and magnetizing current

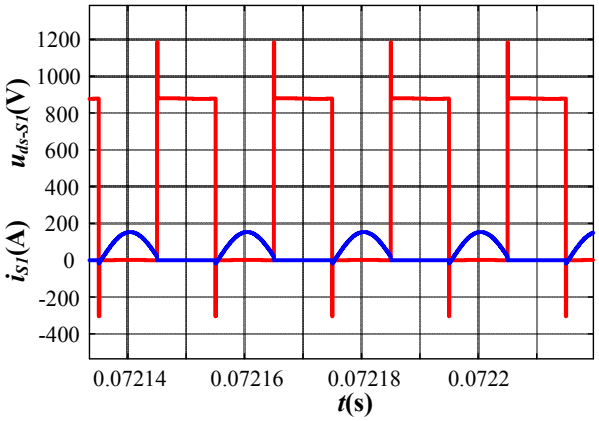

Fig. 11. The drain-source voltage and current of MOSFET S_1

B. Experimental Verification

A 30kW prototype based on all SiC devices is built to demonstrate the practicability of the proposed converter, as shown in Fig. 12. And its parameters are the same as the parameters of the simulation, which are listed in Table I. The power circuit of this prototype is mainly constructed by copper bars on account of high power and high voltage. The prototype has been tested and experimental waveforms are shown in Fig. 13-16.

Fig. 12. Experimental prototype of the IB-FBLLC converter

Fig. 13 shows the input current waveform (2), input voltage waveform (1), intermediate stage voltage

waveform (3) and output voltage waveform (4). The input current ripples are greatly decreased compared to primitive Boost converter because the phase-shifted drive signal shifts the peak and valley values of the two-phase inductor current ripple. The voltage achieves a 10x conversion. The DC bus voltage is stable and there are very few ripples.

Fig. 14 and Fig. 15 show the gate-source and drain-source waveforms of SiC MOSFET S_1 in the back-stage. The back-stage full-bridge LLC topology is able to achieve soft-switching including ZVS of primary switches and ZCS of secondary diodes. The voltage on the switch has dropped to zero before the switch is turned on. The current through the diode has dropped to zero before the switch is turned off. They result in a significant reduction in switching losses.

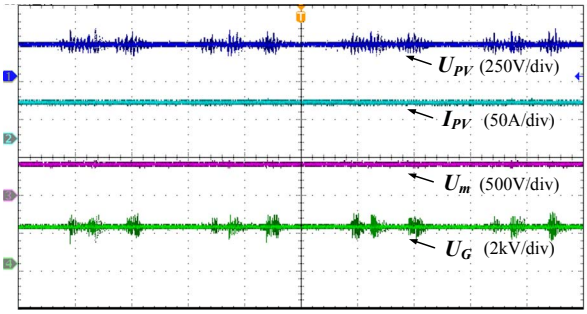

Fig. 13. Current waveform of PV side and voltage waveforms at various levels

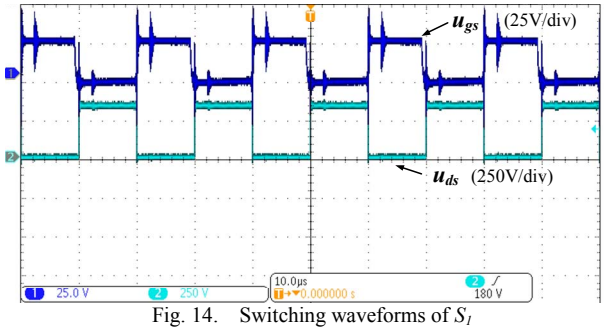

Fig. 14. Switching waveforms of S_1

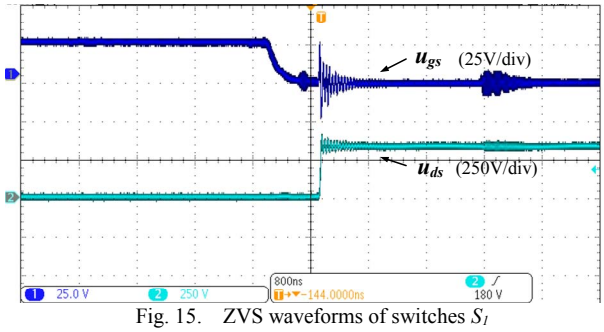

Fig. 15. ZVS waveforms of switches S_1

Fig. 16 shows the voltage and current waveforms of the resonant tank. The magnetizing inductor current waveform is in a zigzag shape. The resonant inductor current is nearly completely sinusoidal. In this case, the switching frequency f_s is equal to the first resonant frequency f_r of the network composed of the resonant inductor and the resonant capacitor, and the magnetizing inductor does not participate in the resonance.

Fig. 17 shows the dynamic response when input voltage rises. When the PV side input voltage rises in steps of 40V, the DC bus voltage remains stable and unchanged. Experimental results indicate that IB-FBLLC performs well regardless of steady state or dynamic performance.

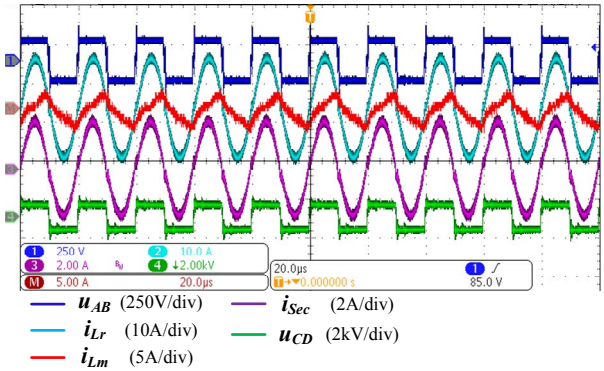

Fig. 16. Measured steady-state resonant waveforms

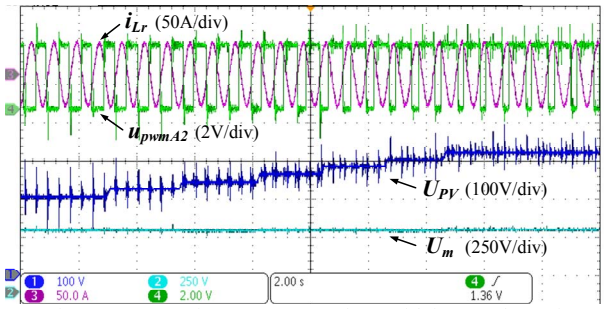

Fig. 17. Dynamic response waveform with input voltage rise

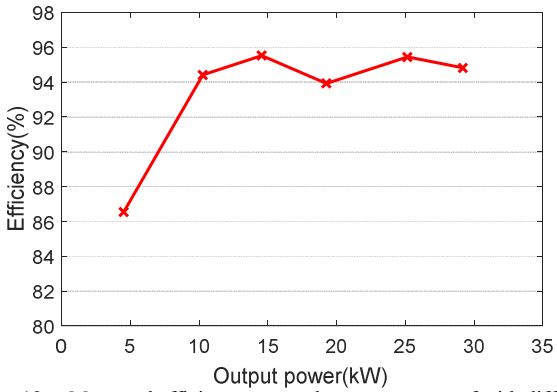

Fig. 18. Measured efficiency versus the output power of with different output voltages

The efficiency curve of IB-FBLLC converter is tested and plotted in Fig. 18. The system efficiency is calculated by $\eta = P_o / (P_{in} + P_{aux})$, where P_o is the output power, P_{in} is the input power, and P_{aux} is the power consumption of the auxiliary circuits. The experimental data is measured by a high-precision power analyzer. It is shown that high efficiency can be achieved because of soft-switching. The peak efficiency of IB-FBLLC converter is 95.527%.

V. Conclusions

In this paper, requirements for the converter module in MVDC grid-connected PV system applications are

explored deeply. Based on these requirements, an isolated high step-up DC-DC converter IB-FBLLC is proposed. The switching frequency can be increased on account of the use of SiC MOSFETs and soft-switching. Also, the input current ripples are reduced significantly due to the interleaved technique. Apart from this, the conversion efficiency is improved significantly because of soft-switching. Experimental results show that IB-FBLLC converter is characterized by a high step-up ratio and high efficiency.

ACKNOWLEDGMENT

The authors would like to acknowledge the supports by National Key R&D Program of China (2016YFB0900205), National Natural Science Foundation of China (51577102, 51811540405).

REFERENCES

[1] J. Echeverria, S. Kouro, M. Pérez, and H. Abu-Rub, "Multi-modular cascaded DC-DC converter for HVDC grid connection of large-scale photovoltaic power systems," in *IECON 2013-39th Annual Conference of the IEEE Industrial Electronics Society*, Vienna, 2013, pp. 6999-7005.

[2] H. Choi, M. Ciobotaru, M. Jang and V. G. Agelidis, "Performance of Medium-Voltage DC-Bus PV System Architecture Utilizing High-Gain DC–DC Converter," *IEEE Trans. Sustainable Energy*, vol. 6, no. 2, pp. 464-473, Apr. 2015.

[3] J. Robinson, D. Jovcic, and G. Joos, "Analysis and design of an offshore wind farm using a MV DC grid," *IEEE Trans. Power Del.*, vol. 25, no. 4, pp. 2164-2173, Oct. 2010.

[4] H. Hu, Q. Shi, Z. He, J. He, and S. Gao, "Potential harmonic resonance impacts of PV inverter filters on distribution systems," *IEEE Trans. Sustainable Energy*, vol. 6, no. 1, pp. 151-161, Jan 2015.

[5] C. A. Rojas, S. Kouro, M. A. Perez, and J. Echeverria, "Dc-dc mmc for HVDC grid interface of utility-scale photovoltaic conversion systems," *IEEE Trans. Ind. Electron.*, vol. 65, no. 1, pp. 352-362, Jan. 2018.

[6] Y. Wang, C. Ju, H. Wang, and S. Meng, "Design and control of dc-dc grid-connected converter for photovoltaic power," in *31st European Photovoltaic Solar Energy Conference and Exhibition*, 2014, pp. 2353-2357.

[7] R. E. Torres-Olguin, M. Molinas, and T. Undeland, "Offshore wind farm grid integration by VSC technology with LCC-based HVDC transmission," *IEEE Trans. Sustainable Energy*, vol. 3, no. 4, pp. 899-907, Oct. 2012.

[8] J. W. Zapata, T. A. Meynard, and S. Kouro, "Partial power DC-DC converter for large-scale photovoltaic systems," in *2016 IEEE 2nd Annual Southern Power Electronics Conference (SPEC)*, Auckland, 2016, pp. 1-6.

[9] Y. Liu, H. Abu-Rub, and B. Ge, "Front-end isolated quasi-z-source DC-DC converter modules in series for high-power photovoltaic systems part i: configuration, operation, and evaluation," *IEEE Trans. Ind. Electron.*, vol. 64, no. 1, pp. 347-358, Jan. 2017.

[10] X. Huang, H. Wang, L. Guo, C. Ju, R. Liu, S. Meng, Y. Wang, and H. Xu, "Large-scale photovoltaic generation system connected to HVDC grid with centralized high voltage and high power DC/DC converter," in *2017 20th International Conference on Electrical Machines and Systems (ICEMS)*, Sydney, 2017, pp. 1-6.

[11] Y. T. Chen, S. M. Shiu, and R. H. Liang, "Analysis and design of a zero-voltage-switching and zero-current-switching interleaved boost converter," *IEEE Trans. Power Electron.*, vol. 27, no. 1, pp. 161-173, Jan. 2012.

[12] H. Wang, and Z. Li, "A PWM LLC type resonant converter adapted to wide output range in PEV charging applications," *IEEE Trans. Power Electron.*, vol. 33, no. 5, pp. 3791-3801, May. 2018.

[13] G. Cao, K. Sun, S. Jiang, S. Lu, and Y. Wang, "A modular DC/DC photovoltic generation system for HVDC grid connection," *Chinese Journal of Electrical Engineering*, vol. 4, no. 2, pp. 56-64, Jun. 2018.

[14] X. Fang, H. Hu, Shen, Z. J. Shen, and I. Batarseh, "Operation mode analysis and peak gain approximation of the LLC resonant converter," *IEEE Trans. Power Electron.*, vol. 27, no. 4, pp. 1985-1995, Apr. 2012.

[15] J. Zhang, J. Liu, J. Yang, N. Zhao, Y. Wang, and T. Q. Zheng, "An LLC-LC type bidirectional control strategy for an LLC resonant converter in power electronic traction transformer, " *IEEE Trans. Ind. Electron.*, vol. 65, no. 11, pp. 8595-8604, Nov. 2018.